

1 **Finite Element Modelling of Atomic Force Microscope Cantilever beams**
2 **with Uncertainty in Material and Dimensional Parameters**

3
4 Bin Wang^{1*}, Xiao Wu², Tat-Hean Gan¹ and Alexis Rusinek³

5
6 ¹School of Engineering and Design, Brunel University, UK

7 ²School of Mechanical Engineering, Southwest Jiaotong University, P. R. China

8 ³National Engineering School of Metz, Laboratory of Mechanics, France

9
10 *Corresponding author: Bin Wang, email: bin.wang@brunel.ac.uk; Tel: +44 1895267304

11
12 **Abstract**

13 The stiffness and the natural frequencies of a rectangular and a V-shaped micro-cantilever
14 beams used in Atomic Force Microscope (AFM) were analysed using the Finite Element (FE)
15 method. A determinate analysis in the material and dimensional parameters was first carried
16 out to compare with published analytical and experimental results. Uncertainties in the
17 beams' parameters such as the material properties and dimensions due to the fabrication
18 process were then modelled using a statistic FE analysis. It is found that for the rectangular
19 micro-beam, a $\pm 5\%$ change in the value of the parameters could result in 3 to 8-folds (up to
20 more than 45%) errors in the stiffness or the 1st natural frequency of the cantilever. Such big
21 uncertainties need to be considered in the design and calibration of AFM to ensure the
22 measurement accuracy at the micron and nano scales. In addition, a sensitivity analysis was
23 carried out for the influence of the studied parameters. The finding provides useful guidelines
24 on the design of micro-cantilevers used in the AFM technology.

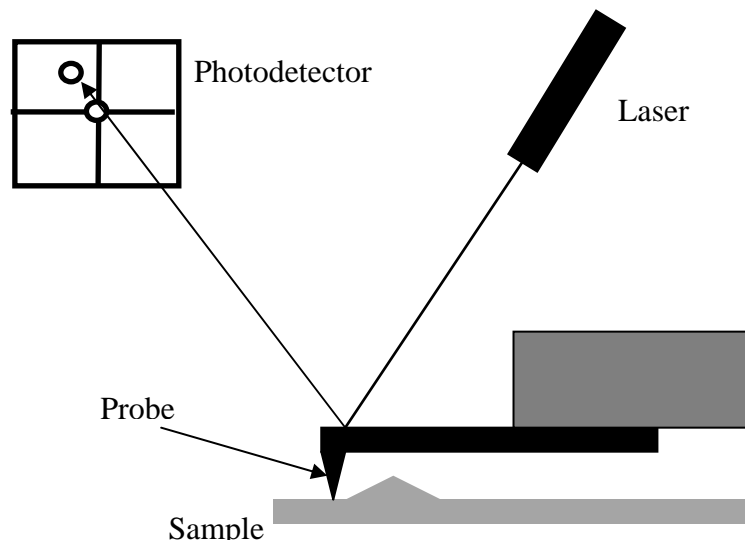
25
26 *Keywords:* Atomic force microscope; cantilever; stiffness; natural frequency; sensitivity
27 analysis

28

29 **1. Introduction**

30 Atomic Force Microscopes (AFMs) have been widely used for scanning measurement at
31 the micron and nano scales. A micro-cantilever with a sharp probe at its free end is a key
32 component of an AFM, as shown in Fig. 1. It works in a way similar to a gramophone stylus.
33 While the probe scans a surface of a sample, the contact force between the probe tip and the
34 surface being scanned leads to a small elastic deflection of the micro-cantilever. The
35 deflection is measured by reflecting a laser beam to a position-sensitive photodetector which
36 records the movement of the reflected laser beam. By converting the signal generated from
37 the photodetector, a topographic image of the scanned surface can be generated.

38 The quality of the image obtained from an AFM is greatly dependent on knowing the
39 elastic parameters of the cantilever. Depending on the mode of application, either the bending
40 stiffness or the 1st natural (resonant) frequency of the cantilever is used. A good knowledge of
41 these, often referred to as the calibration of the cantilever, is of fundamental importance to
42 both the manufacturer and the user as it determines the accuracy of the measurement. Since
43 the invention of AFM, the study of the calibration of AFM cantilevers has been an essential
44 subject in the development of the technology [1].

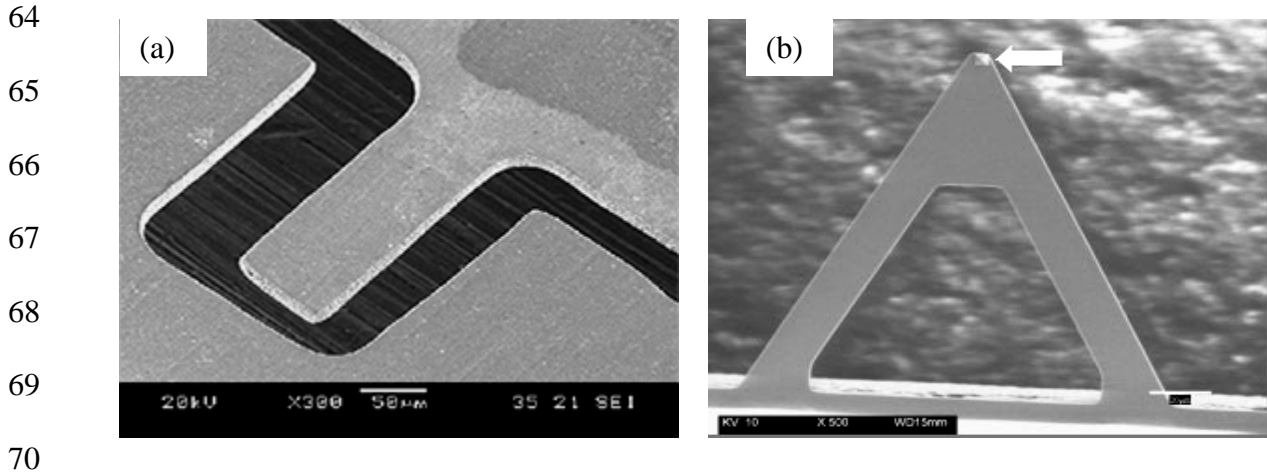


45
46 Fig. 1 The working principle of an AFM

47 An AFM can be used in different modes of measurement, such as contact, noncontact and
48 tapping modes [1-3]. The classification is based on the type of the interaction between the
49 probe tip and the surface being scanned. For the contact mode, the probe touches the sample
50 surface all the time. It is customary to call this type of measurement as the static mode. As a
51 high magnitude contact force may damage the sample surface, a cantilever of a lower
52 stiffness is preferred. A flexible cantilever will also yield in large deformation, leading to
53 higher measurement sensitivity.

54 An AFM can also be used in a non-contact and tapping manner as termed the dynamic
55 mode. In the dynamic mode, the cantilever is externally oscillated at or close to its 1st natural
56 frequency about 5 to 10 nano-meter above the sample surface such that the probe only comes
57 in contact with the sample once in each vibration cycle. Changes in the frequency due to the
58 contacts provide information of the sample surface profile. In this mode, a higher stiffness, or
59 higher natural frequencies, normally only the 1st one being used for resonance response,
60 would give more accurate results.

61 There exist a variety of shapes for AFM cantilevers which are used in different modes for
62 different applications. The most commonly used ones are the rectangular and the V-shaped
63 configurations, as shown in Fig. 2.



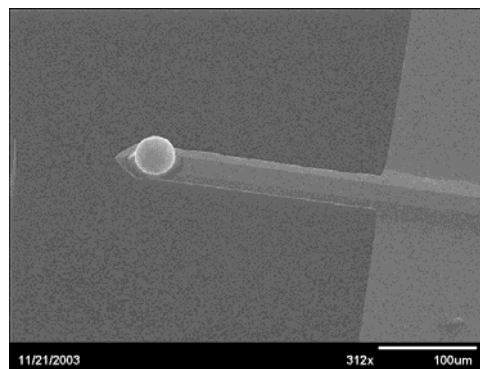
71 Fig. 2 SEM (Scanning electron microscope) images of (a) a rectangular cantilever and (b) a
72 V-shaped cantilever. The arrow in (b) indicates the probe tip. A better view of the tip is
73 shown in Fig. 6

74

75 AFM cantilevers are mostly made of silicon and silicon nitride in a microelectronic
76 fabrication process. Cantilevers are made by first patterning a circular silicon dioxide dot on a
77 silicon wafer. Silicon beneath the silicon dioxide dot is then etched, undercut and oxidized.
78 Subsequently, the silicon post becomes a tip after the removal of the oxide. Then, the
79 cantilever is formed by etching the boron doped silicon [1, 2].

80 The micro-fabrication process, however, often leads to variable stoichiometry of the
81 cantilevers, which causes difficulties in controlling the dimensions of the cantilever, such as
82 the thickness and the length, as well as in ensuring the value of the material properties, such
83 as the Young's modulus and the density. All these will cause variation in the stiffness and the
84 natural frequencies of fabricated cantilevers [4].

85 To obtain the value of the stiffness and the natural frequencies of the cantilever, both
86 experimental and analytical approaches have been proposed. For the measurement of the
87 stiffness, the cantilever is pushed at the free end by a force of a known magnitude and the
88 corresponding deflection is measured, from which the stiffness can be calculated based on the
89 classic elastic beam theory. The known force can be produced in different ways. One way is
90 to attach a tungsten sphere [5] of a known mass as shown in Fig. 3. Another commonly seen
91 method is to use a reference cantilever of known stiffness to press against the unknown one.
92 From the deflection of the know cantilever, the interaction force can be determined. This
93 force is then used together with the deflection of the unknown cantilever to determine its
94 stiffness. Such static methods can achieve an accuracy of 2~5% [6].



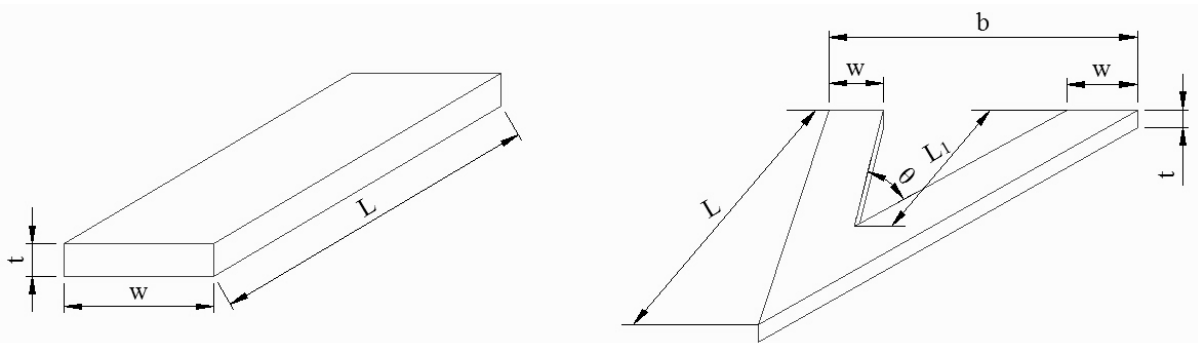
95
96 Fig. 3 A cantilever with a tungsten sphere glued to its free end [8]
97

98 The stiffness can also be determined by dynamic test methods which rely on the
99 determination of the natural frequencies of the cantilever. One method is to fix a mass [7] to
100 the free end then monitoring the change in the natural frequency of vibration. This technique
101 is applicable to any cantilevers. However, as the mass has to be permanently added (to
102 sustain with the vibration) it is destructive and the error in measurement is relatively large [9,
103 10].

104 Apart from experimental measurements, analytical modelling has also been used to derive
105 theoretical values of the stiffness and the natural frequencies based on the classic structural

106 mechanics. For V-shaped cantilevers, different formulae have been proposed, eg. Butt et al.
107 [12], Sader and White [13] and Sader et al. [14]. One of the examples is the Parallel Beam
108 Approximation (PBA) by Albrecht et al. [11] in which the V shape is approximated by two
109 rectangles in parallel. Analytical modelling requires accurate knowledge of the cantilever
110 properties, such as the Young's modulus and the geometry, with the latter usually measured
111 from scanning electron micrograph (SEM).

112 The structural geometry parameters of a rectangular and a V-shaped cantilever are shown
113 in Fig. 4, with notations indicating the dimensional parameters needed in determining the
114 mechanical performance of the cantilever.



115
116 Fig. 4 Geometric parameters of the rectangular and V-shaped cantilevers (the probe tip at
117 the free end is ignored as negligible in affecting the mechanical performance)

118
119 AFM cantilevers are typically very thin and SEM measurement accuracy error can be of
120 3%. This may lead to errors in calculation as the thickness is of 3rd power in beam deflection
121 formula. In addition, material constants such as the Young's modulus may also vary due to
122 the anisotropic deposit of the thin film, to a variation range typically more than 3% [13].

123 In this work, we are motivated to use the finite element (FE) method as an alternative
124 approach to obtain the stiffness and the natural frequencies of an AFM cantilever, and to
125 introduce a range of randomness to the numerical model to examine the influence of the
126 uncertainties in the material and dimensional parameters of the cantilever. The FE model will

127 also allow a sensitivity study to be carried out to determine the significance of the parameters
128 involved.

129 Both the dynamic and static FE models were built for a rectangular and V-shaped
130 cantilever, respectively. The paper is organised in the following order. First a deterministic
131 FE analysis is discussed to verify the FE outcomes with published theoretical and
132 experimental results. Then the variation in the beam dimensions and the Young's Modulus
133 are introduced, assuming a uniform random distribution in the values of the parameters such
134 as the geometric and the Young's modulus between $\pm 5\%$ of their nominal values. Finally a
135 sensitivity analysis was carried out to obtain the influential effect of the parameters on the
136 stiffness and the 1st natural frequency of the cantilever.

137

138 **2. Finite element analysis**

139 A commercial finite element code ANSYS (Ansys Inc.) was used to model the micro-
140 cantilevers. The nominal values of the parameters used in the simulations were obtained from
141 a manufacturer of the cantilevers, for instance, AC-160 tapping mode rectangular cantilever
142 shown in Figs. 5 and 6 by Olympus Corporation [16]. These include both the dimensions and
143 the material properties, as listed in Table 1.

144 Measurements of the physical dimensions were also performed using SEM [8]. The
145 average length and width are 159.6 μm and 51.28 μm , respectively, with the uncertainty
146 relative to the nominal value being less than 1%. The thickness of the cantilever is critical for
147 bending deflection, and the uncertainty was found to be much higher. Compared to the
148 nominal value of 4.6 μm , the measured thickness varies from 3.84 to 4.97 μm (corresponding
149 error -16.5% and 8%), respectively. In the FE model, an average thickness of 4.88 μm was
150 used based on SEM measurement.

151

152
153
154
155
156
157
158
159
160
161
162

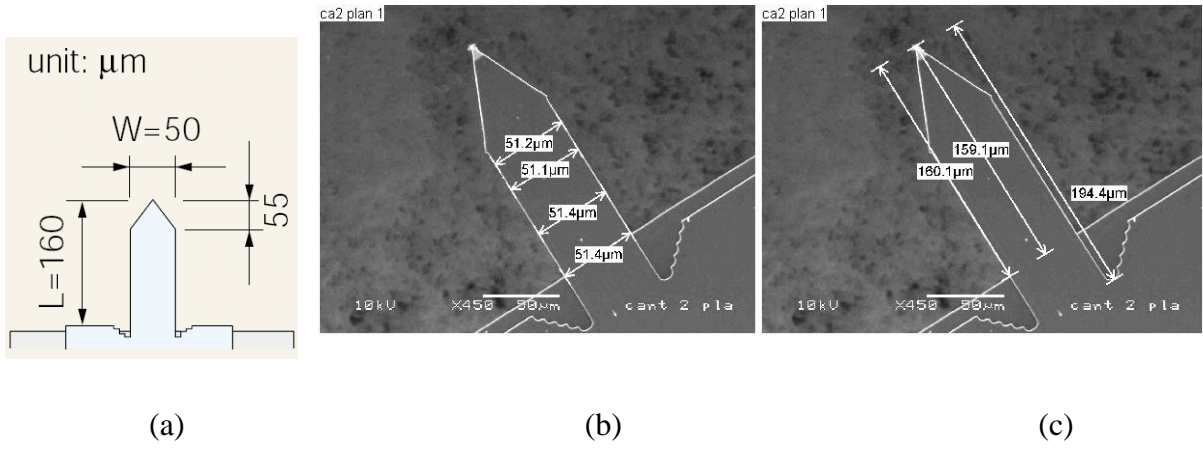


Fig. 5 (a) The manufacturer's dimensions of the AC-160 micro cantilever [16], (b) and (c) SEM images of plane view dimensions [8]

163
164
165
166
167

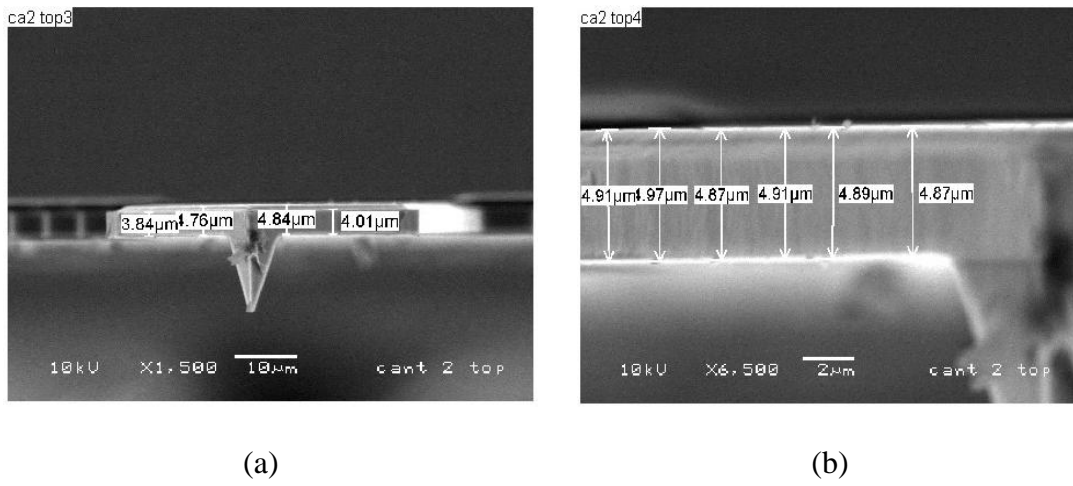


Fig. 6 SEM images of the thickness of the cantilever [8] (a) View in the axial direction at the free end, (b) close-up side view of the cantilever root

168 The value of the Young's modulus, density, Poisson's ratio and geometric parameters used
169 in the FE analysis are listed in Table 1 for the rectangular configuration and Table 2 for the
170 V-shaped one. To cater for the variation in the parameters, a randomness of uniform
171 distribution in dimensions and the Young's modulus were introduced in a range of $\pm 5\%$ of

172 the corresponding nominal values. The density and Poisson ratio were assumed constant due
 173 to lack of available data. The nominal values of the parameters (either the average of the
 174 measurement, or the value provided by the manufacturer) were used in a deterministic
 175 analysis first to verify the FE model with literature results. The cantilevers were assumed to
 176 be isotropic and homogeneous, with one end fully clamped as the boundary condition.

177

178 Table 1 Inputs of the FE model for the rectangular cantilever

Parameters	Nominal value	Min. value (-5%)	Max. value (+5%)
Length L (μm)	160	152	168
Width W (μm)	50	47.5	52.5
Thickness t (μm)	4.6	4.37	4.83
Young's Modulus E (GPa)	167.4	159.0	175.8
Density ρ ($\text{kg}/\mu\text{m}^3$)	2.33×10^{-15}		
Poisson's ratio ν	0.27		

179

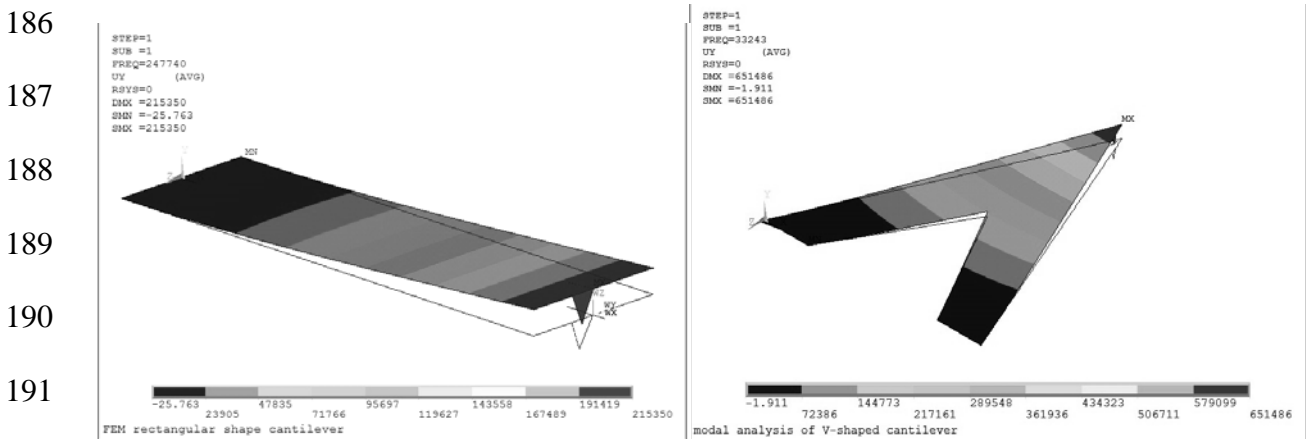
180 Table 2 Inputs of the FE model for the V-shaped cantilever

Parameters	Nominal value	Min. value (-5%)	Max. value (+5%)
Length L (μm)	190	180.5	199.5
Length L_1 (μm)	87.5	83.125	91.875
Width b (μm)	165	156.75	173.25
Single limb width w (μm)	33.3	31.635	34.965
Thickness t (μm)	0.6	0.57	0.63
Young's Modulus E (GPa)	179.0	170.1	188.0
Density ρ ($\text{kg}/\mu\text{m}^3$)	2.33×10^{-15}		
Poisson's ratio ν	0.27		

181

182 The models were built using a quadrilateral shell element provided by ANSYS. After a
 183 convergence test, approximately 27000 elements were used for the rectangular model and

184 46000 elements for the V-shaped cantilever model. Fig. 7 illustrates an example of the output
 185 of dynamic analyses of both configurations.



(a) (b)

194 Fig. 7 The first mode of free vibration of (a) the rectangular cantilever and (b) the V-shaped
 195 cantilever

196 **2.1 Rectangular cantilever**

197 *Dynamic FE modelling for natural frequencies*

198 For the modal analysis of the rectangular cantilever, the first three modes are shown in
 199 Table 3. The nominal frequency values listed in the table indicate the frequencies obtained
 200 with the nominal values of the parameters, while the minimum and maximum are the
 201 frequencies from the corresponding minimum (95% of the nominal) and maximum (105%)
 202 input parameters as listed in Table 1. The percentage values in brackets in Table 3 are the
 203 differences to the nominals. It is clearly shown that the ranges of difference from -16.1% to
 204 19.4% are much bigger than the 5% variation in the input parameters.

205

206 Table 3 First three natural frequencies of the rectangular cantilever

Mode	Deformation	Natural Frequency (kHz)		
		Nominal	Minimum	Maximum
1 st	Flexure	247.74	207.83 (-16.1%)	295.73 (19.4%)

2 nd	Flexure	1546.9	1299.1 (-16.0%)	1750.0 (13.1%)
3 rd	Torsion	1607.7	1480.1 (-7.9%)	1845.0 (14.8%)

207

208 The stiffness k can be calculated analytically from the first natural frequency,

209
$$k = (2\pi f_0)^2 m_e \quad (1)$$

210 where f_0 is the first natural frequency of the cantilever vibration. The effective mass m_e is
 211 equal to the multiplication of the cantilever mass m and a geometrical factor n . n is proposed
 212 as 0.2427 by Sader *et al* [9], or 0.25 by Cleveland *et al* [7]. Table 4 shows the value of the
 213 stiffness from Eqn. (1) and the classic beam theory. Again, big variations are shown from -
 214 16.1% and 49.2% to the nominal values, corresponding to -5% and +5% change in the input
 215 values, respectively.

216

217 Table 4 Stiffness obtained from the 1st natural frequency

		Nominal	Minimum	Maximum
1 st natural frequency (kHz)		247.74	207.83 (-16.1%)	295.73 (19.4%)
Stiffness k (N/m)	Eq. (1) with $n = 0.2427$ [9]	50.42	33.63 (-33.3%)	75.25 (49.2%)
	Eq. (1) with $n = 0.25$ [7]	51.94	34.64 (-33.3%)	77.52 (49.2%)
	Analytical $k = \frac{Et^3w}{4L^3}$	49.73	33.24 (-33.2%)	74.02 (48.8%)

218

219 *Static FE modelling for stiffness*

220 The static method is an alternative way to calculate the stiffness using deflections under
 221 specific loading. In the FE model, a point load of the magnitude of 1 and 10 μ N was applied
 222 perpendicular to the cantilever at its free end. Table 5 gives the deflection and the stiffness
 223 calculated. Note that variations of deflection changes are the opposite sense to those of the
 224 stiffness. The two loads produce identical stiffness under elastic deformation.

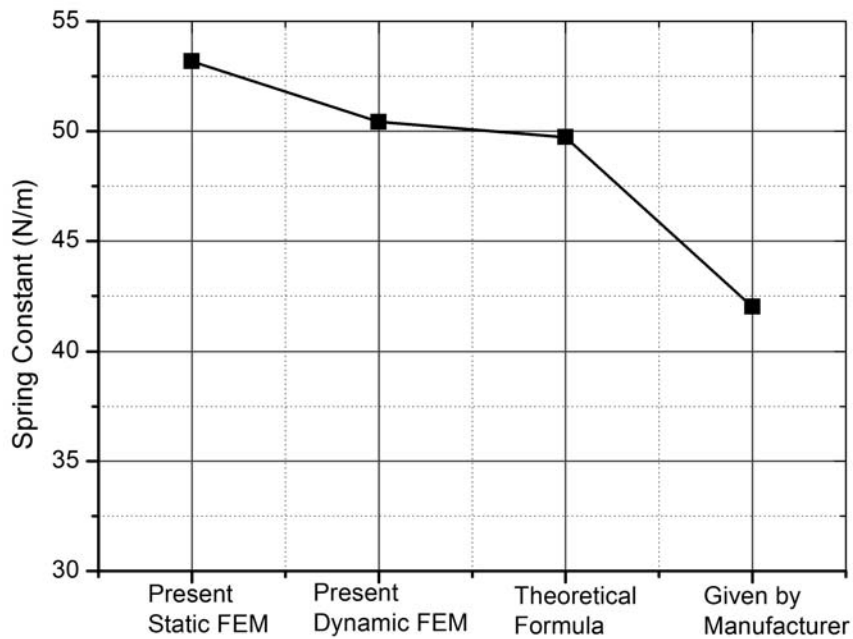
225

226 Table 5 FEA results of the stiffness of the rectangular cantilever model

load		Nominal	Minimum	Maximum
F=1μN	Deflection	0.019	0.028 (48.7%)	0.012 (-36.8%)
	Stiffness K (N/m)	53.180	35.759 (-32.8%)	80.302 (51.0%)
F=10μN	Deflection	0.188	0.280 (48.9%)	0.125 (-33.5%)
	Stiffness K (N/m)	53.180	35.759 (-32.8%)	80.301 (51.0%)

227

228 The stiffness is given as 53.18 N/m by the static FEM, 49.73 N/m by the analytical
 229 modelling, 50.42 N/m by the dynamic FEM and 42 N/m by the manufacturer, as compared is
 230 in Fig. 8. It shows that both FE models and the theoretical method agree well, but with a
 231 notable difference (more than 20%) to the value provided by the manufacturer.



232

233 Fig. 8 Comparison of the stiffness of the rectangular cantilever obtained by different methods

234

235 2.2 V-shaped Cantilevers

236 For the V-shaped cantilever, a randomness variation of $\pm 5\%$ was also introduced in the
 237 input value of the parameter. Results of the dynamic FEM for the nominal, minimum and

238 maximum values are shown in Table 6. The “magnified” errors in the natural frequencies are
 239 given in brackets.

240 Table 6 The first five natural frequencies of V-shaped cantilevers and differences to the normal value

Mode	Description	Natural Frequency (kHz)		
		Nominal	Minimum	Maximum
1 st	Flexure	33.243	26.939 (-19.0%)	41.097 (23.6%)
2 nd	Flexure	171.797	141.644 (-17.6%)	208.652 (21.5%)
3 rd	Torsion	190.727	157.166 (-17.6%)	231.784 (21.5%)

241

242 The first mode is compared with the theoretical result and experimental measurement [5]
 243 as given in Table 7, showing an error range within 8% for the 1st mode and 14% for the 2nd.

244 Table 7 Comparison of the 1st natural frequencies from theory, experimental [5] and FEA

Theoretical (kHz)	Experimental (kHz)	FEM (kHz)
34	31.5	33.2

245

246 A static FE analysis was also carried out with $\pm 5\%$ error introduced to the input value, as
 247 shown in Table 8. Like in the realiser results, the increased errors are clearly evidential.

248

249 Table 8 FEA results of the stiffness under different loads for the V-shaped beam model

Force		Nominal	Minimum	Maximum
F=1 μ N	Deformation	10.289	14.766 (43.5%)	7.198 (-30.0%)
	Stiffness K	0.0972	0.068 (-30.0%)	0.139 (43.0%)
F=10 μ N	Deformation	102.887	147.659 (43.5%)	71.981 (-30.0%)
	Stiffness K	0.0972	0.068 (-30.0%)	0.139 (43.0%)

250

251 Results of different theoretical models [12-14], the dynamic FEM, and the static FEM
 252 agree well except that of Albrecht [11], as shown in Fig. 9.



253

254 Fig. 9 Comparison of the stiffness of the V-shaped beam obtained by different methods.

255

256 Results of finite element simulations clearly show an increased error bands in the
 257 cantilevers stiffness and natural frequencies due to small variations in the input values of
 258 cantilever dimensions and material property. For design and calibration purpose, the “error
 259 contribution” of each of the input parameters needs to be investigated. In the following
 260 section, a sensitivity study is discussed, aiming to identify the influence of the input
 261 parameters on the overall performance of the cantilevers.

262

263 3. Sensitivity Study

264 3.1. Mathematical model for sensitivity analysis

265 For both the rectangular and V-shaped cantilevers, a 5% variation in the parameter values
 266 leads to much bigger changes in the natural frequencies and the stiffness. From the design
 267 view point, it is useful to know the scale of influence of each parameter on the performance

268 of the cantilevers. In this section, a sensitivity analysis is presented on the significance of the
269 dimension and material parameters.

270 Sensitivity to a variable is defined by the first-order derivative of a function with respect to
271 the variable. For instance, for a multivariate function $f(X)$ with X representing the variable
272 vector of k parameters, $X = (x_1, x_2, \dots, x_k)$, the sensitivity of function f to its j -th parameter x_j
273 can be expressed as

$$274 \quad S_i = \frac{\partial f(X)}{\partial x_j} \quad j = 1, 2, \dots, k \quad (2)$$

275 A higher magnitude of S_j indicates a stronger sensitivity of f to x_i . Note that S_j can be both
276 positive and negative for the correlation of f to x_i .

277 In the static analysis, the global governing equations is

$$278 \quad [K]\{\delta\} = \{F\} \quad (3)$$

279 where $[K]$ denotes the structure's stiffness matrix, $\{\delta\}$ the nodal displacement and $\{F\}$ the
280 external loading.

281 Taking partial derivatives of Eqn. (3) and noticing that the external loading F is
282 independent of the structural and material parameters, thus $\frac{\partial F}{\partial x_j} = 0$, we have

$$283 \quad \frac{\partial \{\delta\}}{\partial x_j} = -[K]^{-1} \frac{\partial [K]}{\partial x_j} \{\delta\} \quad (4)$$

284 From FEA, the nodal displacement $\{\delta\}$ can be calculated. Then the displacement
285 sensitivity $\frac{\partial \{\delta\}}{\partial x_j}$ can then be obtained from equation (4).

286 For the dynamic analysis, the equation of free vibration can be expressed as

$$287 \quad [K] - \lambda_i [M] \{\varphi_i\} = 0 \quad i = 1, 2, \dots, n \quad (5)$$

288 where $[M]$ is the mass matrix; λ_i the i -th eigenvalue of the natural frequency, $\{\varphi_i\}$ the i -the
 289 order eigenvectors; and n the total number of degree of freedom.

290 Taking partial derivative of Eq. (5) with respect to the parameter x_j yields in

$$291 \left(\frac{\partial[K]}{\partial x_j} - \frac{\partial \lambda_i}{\partial x_j} [M] - \lambda_i \frac{\partial[M]}{\partial x_j} \right) \{\varphi_i\} = 0 \quad (6)$$

292 Multiplying Eqn. (6) on the left by $\{\varphi_i\}^T$ and introducing a generalized mass
 293 $m_i = \{\varphi_i\}^T [M] \{\varphi_i\}$, the sensitivity of the i -th order eigenvalue λ_i with respect to the j -th
 294 parameter x_j is

$$295 \frac{\partial \lambda_i}{\partial x_j} = \frac{\{\varphi_i\}^T \left(\frac{\partial[K]}{\partial x_j} - \lambda_i \frac{\partial[M]}{\partial x_j} \right) \{\varphi_i\}}{m_i} \quad (7)$$

296 The variation of input parameters in this study was limited within the range from -5% to
 297 +5% of their nominal values and was chosen randomly based on the uniform distribution
 298 assumption. After the value of the parameters was randomly chosen, a finite element
 299 simulation was carried out. From the FE results, the sensitivity data was calculated from Eqns.
 300 (4) and (7). This is virtually a Monte Carlo approach when dealing with uncertainty in
 301 variables.

302 A commercial code Isight (Dassault Systems Co) was used for the sensitivity study in
 303 connection with ANSYS. Isight picks up parameter values based on random sampling for
 304 each parameter in a uniform distribution. The chosen values were then used by ANSYS for
 305 simulation. The obtained FE results are then used by the Isight again to calculate the partial
 306 derivatives to obtain the sensitivity of the stiffness or the 1st natural frequency on individual
 307 input parameter.

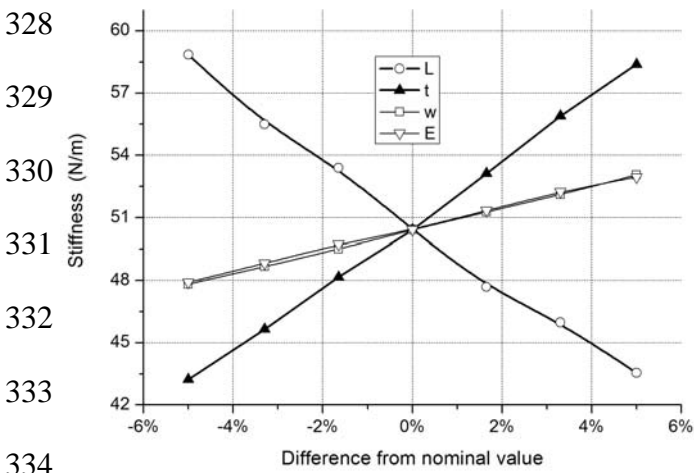
308

309 **3.2. Sensitivity analysis results**

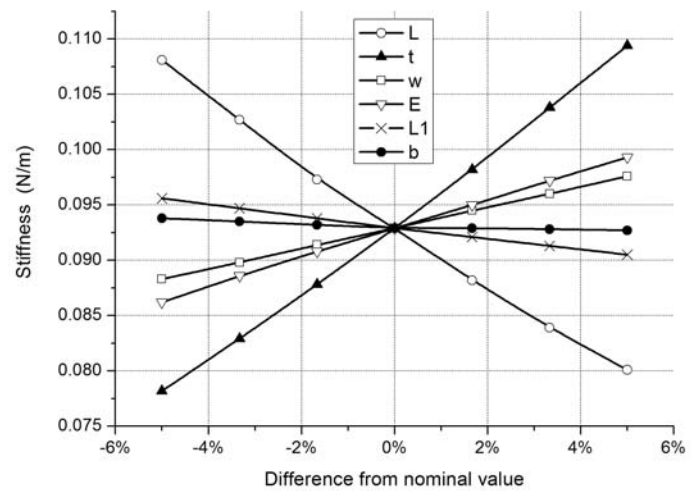
310 The effect of the input parameter variables on the stiffness and the first natural frequencies
 311 were obtained, as given in Fig. 10, for both the rectangular and V-shaped micro-cantilevers.
 312 The notations of the legends are defined in Fig. 4. In Fig. 10, the horizontal axes shows the
 313 range of variations of the input parameters, and the vertical axes give the value of the
 314 magnitude of the stiffness or the 1st natural frequency. The influence appears to be all linear
 315 approximately, due to the narrow range of variation.

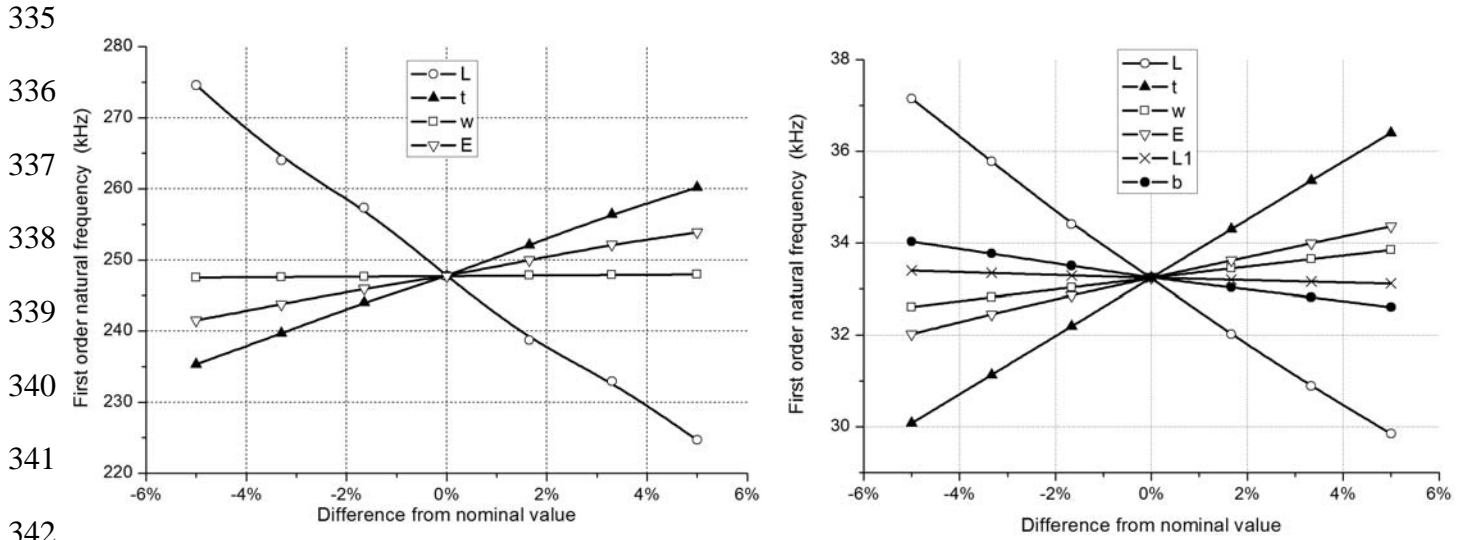
316 For the rectangular cantilever in Fig. 10(a), the cantilever length L has the biggest impact
 317 overall on both the stiffness and the 1st natural frequency with negative slopes, meaning that
 318 an increase in the length will lead to a reduction in the stiffness and the 1st natural frequency
 319 (ie. negative correlation). This is expected from the classic beam theory as the flexural
 320 behaviour of a cantilever is reversely proportion to the length of a beam. Useful conclusions
 321 can be drawn from the figure. For instance, we can see that for every 1% increase in the
 322 cantilever's length, the natural frequency is reduced by approximately 5.0 Hz. For every 1%
 323 increase in beam thickness, the natural frequency is increased by 2.5Hz. The values of the
 324 slope of these linear relationships in Fig. 10 are given in Table 9 for the significance of the
 325 influence of each parameter.

326
 327



332





(a) Rectangular cantilevers

(b) V-shape cantilevers

Fig. 10 Effect of input parameters on the stiffness and the 1st natural frequency. Parameter notations are defined in Fig. 4.

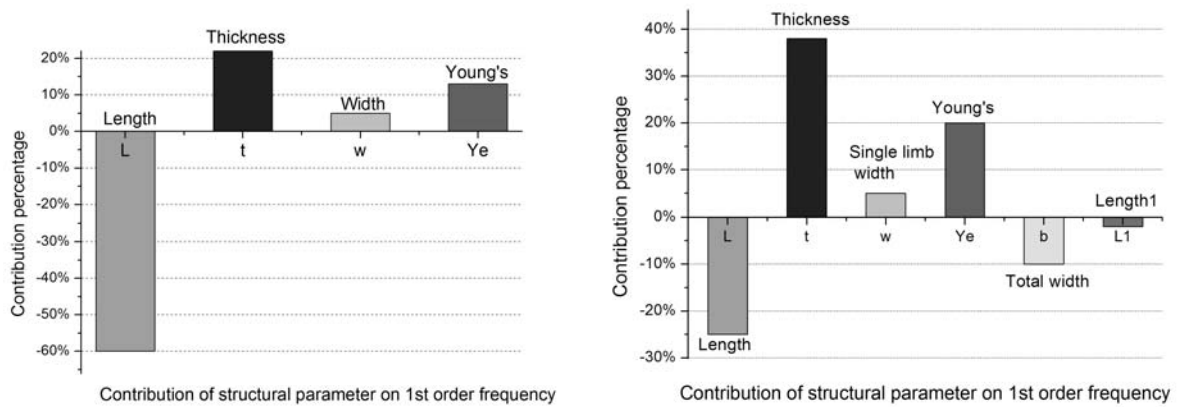
Table 9 variation of the 1st natural frequency and the stiffness to 1% change of each input parameter's nominal value

		L	t	w	E	L_1	b
Rectangular	1 st Natural frequency (kHz)	-4.98	2.49	0.04	1.24		
	Stiffness (N/m)	-1.53	1.52	0.52	0.50		
V-shaped	1 st Natural frequency (kHz)	-0.73	0.39	0.12	0.23	-0.03	-0.14
	Stiffness (N/m)	-0.003	0.003	0.001	0.001	-0.001	-0.0001

A pareto diagram is constructed in Fig. 11 to show the contribution of influence of the input parameters to the 1st natural frequency, as against the overall influence (100%) by all parameters. Fig. 11(a) shows that the contribution rate of the length L is found to be approximately 60%, and in the negative correlation, while the thickness is the next most influential parameter for the rectangular beam.

It is interesting to see that the thickness t has a much stronger effect for the V-shaped cantilever, as seen in Fig. 11(b), even more than that of the length. Considering the difficulty

356 in controlling the thickness in the fabrication process and in its measurement (in comparison
 357 to the length L), this should be the parameter of utmost significance for the design,
 358 fabrication and calibration of the macro-cantilever in AFM. It is also noted that the Young's
 359 modulus has a bigger effect proportionally for the V-shaped cantilever than that for the
 360 rectangular one (20% vs. 13%). It shows that different strategies should be adopted in
 361 selecting parameters for the design and fabrication of different cantilevers.



368 (a) Rectangular cantilevers

368 (b) V-shape cantilevers

369 Fig. 11. Contribution percentage of main parameters on the 1st natural frequency

371 4. Conclusions

372 The finite element method was used to calculate the stiffness and the natural frequencies of
 373 two micro-cantilevers commonly used in AFM. The dependence of the behaviour of the
 374 rectangular and V-shaped cantilevers on the uncertainty of their dimensional and material
 375 parameters was studied. The error limit in this study was set at $\pm 5\%$ of the nominal value of
 376 the parameters which are either the average of the measurement or the one provided by the
 377 manufacturer. FE simulations show that the stiffness and 1st natural frequency of both
 378 cantilevers vary at a much bigger range than the randomness limit introduced in the design
 379 parameters. In order to enhance modelling accuracy, the measurement precision of the

380 dimensional parameters must be improved and variations in material properties need to be
381 minimised though strictly controlled fabrication process.

382 A sensitivity analysis was used to study the influence of design parameters on the 1st
383 natural frequency and the stiffness. It was found that the main factors affecting the accuracy
384 are the length, the thickness, and the Young's modulus, among others. The cantilever length
385 L has the greatest impact on the natural frequency and the stiffness, and is in a negative
386 correlation. In terms of significance, the thickness of the cantilever t is the second parameter,
387 and the Young's modulus E third, affecting the natural frequency with a positive correlation.

388 For the V-shaped cantilever, the cantilever thickness t affects the natural frequency most in
389 a positive correlation. This is followed by the length L in a negative correlation. The effect of
390 the Young's modulus is similar to that of a rectangular cantilever.

391 In this study, approximation was taken for a simplified fully clamped boundary condition.
392 Moreover, the material is assumed homogeneous and isotropic, which is questionable. For
393 instance, growth lines across the thickness of silicon deposits can be seen in Fig. 5, which
394 may contain oriented textures or defects, resulting in non-homogeneity. All these may
395 contribute to the relatively large difference between the measured and modelled results. This
396 remains to be further studied.

397 This study provides a clear understanding on the influence of the uncertainty of influential
398 parameters on the behaviour of micro cantilevers used in the AFM technology. It provides
399 useful insights and guidance for the design and calibration of micro cantilevers in AFM.

400

401 **Acknowledgements**

402 Data and information provided by C. T. Gibson of the University of Leeds is high
403 acknowledged.

404 The research was supported by Sichuan International Research Collaboration Project
405 (2014HH0022).

406

407

408 **References**

409 [1] G Binnig, C F Quate and C Gerber, Atomic force microscope. *Physical Review Letter*,
410 1986; 56 (9):930–933.

411 [2] CB Prater, HJ Butt and PK Hansma, Atomic force microscopy. *Nature*, 1990; 345(6):
412 839-840.

413 [3] J Nader and L Karthik, A review of atomic force microscopy imaging systems:
414 application to molecular metrology and biological sciences. *Mechatronics*, 2004;
415 14(8):907-945.

416 [4] M Tortonese, Cantilevers and tips for atomic force microscopy. *Park Scientific*
417 *Instruments*, 1997; 16(2):28-33.

418 [5] TJ Senden and WA Ducker, Experimental determination of stiffnesss in atomic force
419 microscopy. *Langmuir*, 1994; 10(4): 1003-1004

420 [6] CT Gibson, GS Watson and S Myhra. Determination of the stiffnesss of probes for force
421 microscopy/spectroscopy. *Nanotechnology*, 1996; 7(9): 259-262.

422 [7] JP Cleveland, S Manne, D Bocek and PK Hansma, A nondestructive method for
423 determining the stiffness of cantilevers for scanning force microscopy, *Review of Science*
424 *Instruments*, 1993; 64(2):403-405.

425 [8] CT Gibson, Private communication, Department of Physics and Astronomy, University of
426 Leeds.

427 [9] JE Sader, I Larson, P Mulvaney and LR White, Method for the calibration of atomic
428 force microscope cantilevers, *Review of Science Instruments*, 1995; 66(7):3789-3798.

- 429 [10] CT Gibson, DA Smith and CJ Roberts, Calibration of silicon atomic force microscope
430 cantilevers, *Nanotechnology*, 2005; 16(2):234-238.
- 431 [11] TR Albrecht, S Akamine, TE Carver, and CF Quate. Microfabrication of cantilever styli
432 for the atomic force microscope, *Journal of Vacuum Science & Technology A*, 1990;
433 8(4):3386-3396.
- 434 [12] HJ Butt et al, Scan speed limit in atomic force microscopy, *Journal of Microscopy*, 1993;
435 169(1):75-84
- 436 [13] CA Clifford and MP Seah, The determination of atomic force microscope cantilever
437 stiffness via dimensional methods for nanomechanical analysis. *Nanotechnology*,
438 2005; 16 (9):1666-1880.
- 439 [14] JE Sader, Parallel beam approximation for V-shaped atomic force microscope
440 cantilevers. *Review of Science Instruments*, 1995; 66 (9):4583-4587.
- 441 [15] RD Cook. *Finite Element Modelling for Stress Analysis*. John Wiley & Sons Inc Press,
442 1995, ISBN 0-471-10774-3.
- 443 [16] Olympus Optical Corporation, Tokyo, Japan
- 444 [17] VJ Morris, AR Kirby and AP Gunning, *Atomic Force Microscopy for Biologists*,
445 Imperial College Press, 1999, ISBN 1-86094-199-0.
- 446 [18] GY Chen, RJ Warmack, TThundat and DP Allison, and A Huang, Resonance response
447 of scanning force microscope cantilevers. *Review of Scientific Instruments*, 1994; 65
448 (8):2532-2537.
- 449 [19] MF Ashby, *Materials selection in mechanical design*, Cambridge University Press, 2005,
450 ISBN 0-7506-4357-9.
- 451 [20] M Barbato and JP Conte, Finite element response sensitivity analysis: a comparison
452 between force-based and displacement-based frame element models, *Computer
453 Methods in Applied Mechanics and Engineering*, 2005; 194(8):1479-1512.

- 454 [21] S Wang, Y Sun and RH Gallagher, Sensitivity analysis in shape optimization of
455 continuum structures, *Computer & Structures*, 1985; 20(5):855-867.
- 456 [22] JE Mottershead, M Link and MI Friswell, The sensitivity method in finite element model
457 updating: A tutorial. *Mechanical Systems and Signal Processing*, 2011; 25(10): 2275–
458 2296.
- 459 [23] GD Pollock and AK Noor, Sensitivity analysis of the contact/impact response of
460 composite structures, *Computers & Structures*, 1996; 61(10):251-269.
- 461 [24] JM Pajot and K Maute, Analytical sensitivity analysis of geometrically nonlinear
462 structures based on the co-rotational finite element method, *Finite Elements in Analysis
463 and Design*, 2006; 42(6):900-913.
- 464 [25] KL Reed, KA Rose and RC Whitmore, Latin hypercube analysis of parameter sensitivity
465 in a large model of outdoor recreation demand. *Ecological Modelling*, 1984; 24(9):159-
466 169.
- 467 [26] A Olsson, G Sandberg and O Dahlblom, On Latin hypercube sampling for structural
468 reliability analysis, *Structural Safety*, 2003; 25(1):47-68.
- 469 [27] W Liu, *Design of Experiments*, Tsinghua University Press, 2011.
- 470